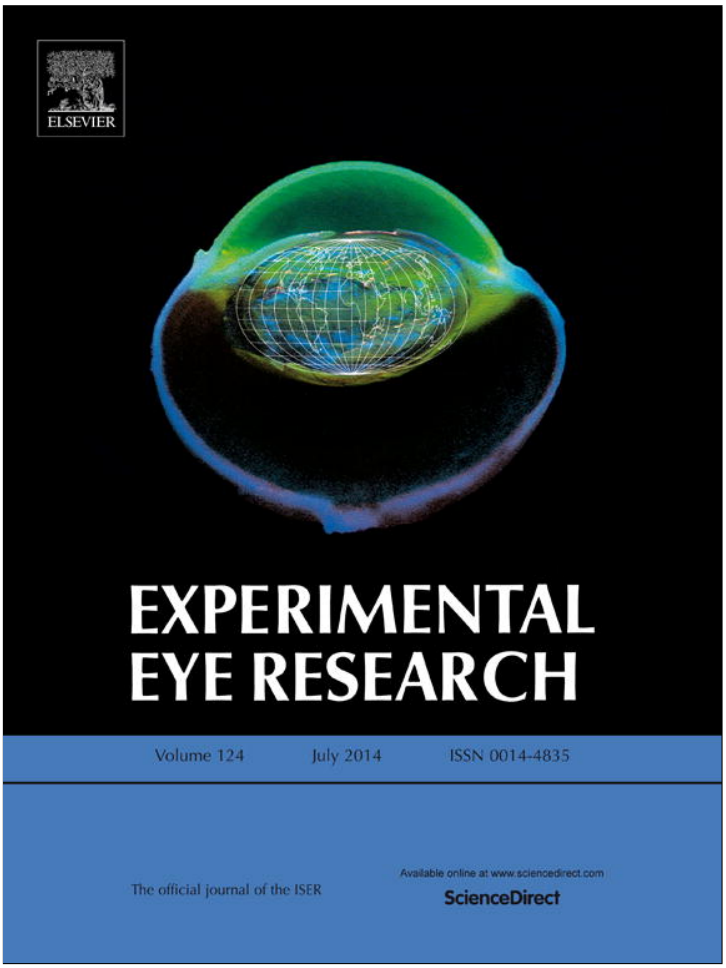

Experimental Eye Research 124 (2014) 37–47

Contents lists available at ScienceDirect

Experimental Eye Research

journal homepage: www.elsevier.com/locate/yexer

Protective effect of a laser-induced sub-lethal temperature rise on RPE cells from oxidative stress

Hisashi Iwami [a], Joachim Pruessner [b], Kunihiko Shiraki [a], Ralf Brinkmann [b,c], Yoko Miura [b,d,*]

[a] Department of Ophthalmology and Visual Science, Osaka City University Graduate School of Medicine, Osaka, Japan
[b] Institute of Biomedical Optics, University of Luebeck, Luebeck, Germany
[c] Medical Laser Center Luebeck, Luebeck, Germany
[d] Department of Ophthalmology, University of Luebeck, Luebeck, Germany

ARTICLE INFO

Article history:
Received 26 January 2014
Accepted in revised form 18 April 2014
Available online 5 May 2014

Keywords:
sub-lethal thermal laser
retinal pigment epithelium
oxidative stress
age-related macular degeneration

ABSTRACT

Recently introduced new technologies that enable temperature-controlled laser irradiation on the RPE allowed us to investigate temperature-resolved RPE cell responses. In this study we aimed primarily to establish an experimental setup that can realize laser irradiation on RPE cell culture with the similar temperature distribution as in the clinical application, with a precise time/temperature history. With this setup, we conducted investigations to elucidate the temperature-dependent RPE cell biochemical responses and the effect of transient hyperthermia on the responses of RPE cells to the secondary-exposed oxidative stress. Porcine RPE cells cultivated in a culture dish (inner diameter = 30 mm) with culture medium were used, on which laser radiation (λ = 1940 nm, spot diameter = 30 mm) over 10 s was applied as a heat source. The irradiation provides a radially decreasing temperature profile which is close to a Gaussian shape with the highest temperature in the center. Power setting for irradiation was determined such that the peak temperature (T_{max}) in the center of the laser spot at the cells reaches from 40 °C to 58 °C (40, 43, 46, 50, 58 °C). Cell viability was investigated with ethidium homodimer III staining at the time points of 3 and 24 h following laser irradiation. Twenty four hours after laser irradiation the cells were exposed to hydrogen peroxide (H_2O_2) for 5 h, followed by the measurement of intracellular glutathione, intracellular 4-hydroxynonenal (HNE) protein adducts, and secreted vascular endothelial growth factor (VEGF). The mean temperature threshold for RPE cell death after 3 h was found to be around 52 °C, and for 24 h around 50 °C with the current irradiation setting. A sub-lethal preconditioning on T_{max} = 43 °C significantly induced the reduced glutathione (GSH)/oxidized glutathione (GSSG) ratio, and decreased H_2O_2-induced increase of intracellular 4-HNE protein adducts. Although sub-lethal hyperthermia (T_{max} = 40 °C, 43 °C, and 46 °C) caused a slight increase of VEGF secretion in 6 h directly following irradiation, secondary exposed H_2O_2-induced VEGF secretion was significantly reduced in the sub-lethally preheated groups, where the largest effect was seen following the irradiation with T_{max} = 43 °C. In summary, the current results suggest that sub-lethal thermal laser irradiation on the RPE at T_{max} = 43 °C for 10 s enhances cell defense system against oxidative stress, with increasing the GSH/GSSG ratio. Together with the results that the decreased amount of H_2O_2-induced 4-HNE in sub-lethally preheated RPE cells was accompanied by the lower secretion of VEGF, it is also strongly suggested that the sub-lethal hyperthermia may modify RPE cell functionality to protect RPE cells from oxidative stress and associated functional decrease, which are considered to play a significant role in the pathogenesis of age-related macular degeneration and other chorioretinal degenerative diseases.

1. Introduction

Photocoagulation on the retina is one of the most established laser therapies in medicine (Meyer-Schwickerath, 1954; Havener, 1964), and has been used for the purpose of inducing positive effects caused by tissue denaturation (Stefánsson, 2006; Gitter, 1975).

* Corresponding author. Institute of Biomedical Optics, University of Luebeck, Peter-Monnik-Weg 4, 23562 Luebeck, Germany. Tel.: +49 451 500 6527; fax: +49 451 500 6546.
E-mail address: miura@bmo.uni-luebeck.de (Y. Miura).

http://dx.doi.org/10.1016/j.exer.2014.04.014
0014-4835/

The first introduction of the therapeutic strategy, in which the laser irradiation is aimed to induce mild hyperthermia in the RPE and the choroid, was the transpupillary thermal therapy (TTT) using 810 nm diode laser, in the treatment of choroidal neovascularization in the patients of age-related macular degeneration (AMD) (Reichel et al., 1999; Ming et al., 2004; Mainster and Reichel, 2000). However, due to the uncertainty of the real tissue damage extent, and due to the appearance of effective pharmaceutical therapies as anti-vascular endothelial growth factor (VEGF) (Zhou and Wang, 2006; Avery et al., 2006), TTT has not been widely used for the treatment of neovascular AMD. Nevertheless, since positive results of TTT on choroidal neovascularization has been reported in recent clinical studies, including low-dose TTT and combination therapy with intravitreal injections (Odergren et al., 2008; Söderberg et al., 2012), it is considered that the low irradiance and low temperature increase has potentially a therapeutic benefit in the treatment of neovascular AMD, although the therapeutic mechanisms of TTT is still unclear (Nowak et al., 2012).

Determination of temperature increase at the retina during laser irradiation for TTT has been enabled by utilizing an optoacoustic method (Kandulla et al., 2006). This technique was further developed for the temperature measurement during retinal photocoagulation and it is already clinically proven (Koinzer et al., 2012; Brinkmann et al., 2012). A feedback control even allows the achievement of a predetermined damage range and strength (Schlott et al., 2012). Very recently, even optical coherence tomography (OCT) can be used to obtain a 3-D time-resolved temperature distribution during photocoagulation (Müller et al., 2012). This technology has raised a new possible therapeutic strategy which may utilize temperature-dependent RPE cell responses, for example, to improve cellular functionality. However, sub-lethal temperature-dependent biochemical response of RPE cells is still very little known to date.

Previous studies on hyperthermia-induced cell responses have been performed frequently by using pre-warmed heating plate or culture medium (Klettner et al., 2012), or temperature-preset incubator (Routt et al., 2011). These methods, however, owing to a very slow temperature rise, are not suitable to study temperature/time-dependent cell response with precise temperature/time control on the second time scale. Moreover, since cultured RPE cells have significantly less melanosomes than in in-vivo condition and the amount of pigmentation varies among cells, clinically-used lasers, as frequency-doubled Nd: YAG lasers (532 nm), are not suitable for in-vitro studies with cultured RPE cells. Thus an optimal in-vitro laser irradiation study model to investigate temperature/time-dependent RPE cell response is required.

We have established a new in-vitro model to study RPE cell responses to laser-induced temperature increase with a precise temperature/time control without any necessity of artificial pigmentation. By using a continuous wave thulium laser at the wavelength of 1.94 μm, which is highly absorbed by the water, a repeatable temperature increase at the cellular level has been enabled. The generated heat by laser absorption at the superior part of the culture medium diffuses to the cells at the bottom of culture dish. Moreover, by adjusting the aiming beam, we created a single laser spot with the diameter of about the same width of the culture dish (30 mm), so that the single laser spot with a similar temperature distribution (Gaussian-like distribution) with a high number of affected cells is created, which enables to perform biochemical investigations on temperature/time-dependent cell responses.

Functional decrease of retinal pigment epithelial (RPE) cell is significantly related to the pathogenesis of many degenerative chorioretinal disorders, such as AMD (Beatty et al., 2000; Mettu et al., 2012; Zarbin, 2004; Chen et al., 2008). Acute and chronic oxidative stresses have been proven to lead to the functional decline of RPE cells, such as junctional disintegrity (Miura and Roider, 2009; Bailey et al., 2004), accumulation of lipofuscin (Roth et al., 2004), excess secretion of angiogenic factors such as VEGF (Schlingemann, 2004), and eventually cell death, mainly through apoptotic pathways (Cai et al., 2000). Lipofuscin accumulation may cause further oxidative damage on RPE cell function (Davies et al., 2001), leading to the accumulation of oxidized lipoprotein and inflammatory cells like macrophages (Schutt et al., 2000) as the components of drusen in sub-RPE space, which is significantly associated with AMD pathogenesis (Roth et al., 2004; Rudolf et al., 2008). Therefore, reducing oxidative stress in RPE cell might decrease the functional impairment of the RPE, eventually the prevention of AMD or other chorioretinal disorders related to RPE cell dysfunction.

Cellular anti-oxidant defense potential is determined significantly by the redox state of glutathione (Meister, 1994; Meister and Anderson, 1983). In healthy cells, reduced glutathione (GSH) accounts for more than 98% of intracellular total glutathione (Kosower NS and Kosower EM, 1978). The ratio of reduced glutathione (GSH) and oxidized glutathione (GSSG) (GSH/GSSG ratio) is widely used as an indicator of cellular redox state (Obin, 1998; Schafer and Buettner, 2001), and a high GSH/GSSG ratio indicates less oxidative damage of the cell. Thus, this ratio plays a critical role in a defense potential of cells against oxidative stress and in the prevention of the development of cell functional disorders.

Oxidative stress, caused by reactive oxygen species (ROS), induces intracellular lipid peroxidation, which leads to the formation of toxic endproducts, as 4-hydroxynonenal (4-HNE) and malondialdehyde (MDA) (Waldeck and Stocker, 1996). They form adducts with DNA, protein, and lipids, and these adducts lead to the functional decrease of intracellular organelles and further lipid peroxidation (Brambilla et al., 1986; Esterbauer et al., 1991). They have been shown to be related to the lipofuscinogenesis in RPE cells and the pathogenesis of AMD (Kaemmerer et al., 2007; Krohne et al., 2010a). Therefore, it is of great importance to reduce intracellular ROS and the eventual formation of these endproducts in RPE cells, by preventing ROS formation or increasing cellular antioxidant defense potential.

We aimed, therefore, to investigate the temperature-dependent RPE cell responses using our original in-vitro irradiation setup, focusing on the subcellular properties regarding cell defense system against oxidative stress. In this study, the effects of the 10 s sub-lethal thermal laser irradiation on the glutathione redox balance (GSH/GSSG ratio) and the oxidative stress-induced 4-HNE generation in RPE cells, as well as the oxidative stress-induced VEGF secretion from RPE cells, were investigated.

2. Materials and methods

2.1. RPE cell culture

Porcine eyes were obtained from a local slaughterhouse, and the RPE cells were isolated as previously described (Yanagihara et al., 1996). Cells were cultivated with dulbecco's modified eagle's medium (DMEM with high glucose 4.5 mg/mL with L-glutamine and sodium pyruvate; PAA, Coelbe, Germany), supplemented with penicillin/streptomycin, and 10% porcine serum (PAA). Cells were incubated at 37 °C under 5% CO_2. Confluent third passage cell cultures were used in all experiments.

2.2. Cell heating system with thulium laser

An experimental setup using a thulium laser (Vela, Starmedtec GmbH, Germany, wavelength: 1.94 μm, power range: 0–20 W) was

established in our laboratory in order to realize sub-lethal to lethal temperature increase on RPE cell culture, which may simulate a temperature profile of a thermal laser spot in clinical use (Fig. 1). The radiation was transmitted by a 0.22 NA 365 μm core diameter fiber (All Silica, Low OH, Cat. No: CF01493-52, Laser Components, Germany). Without any additional imaging optics the culture dish at 12 cm below the fiber tip was irradiated. At this distance the laser spot diameter at the cellular level is 30 mm, which is almost equivalent to inner diameter of the cell culture dish. The irradiation time was fixed to 10 s.

Thulium laser radiation is strongly absorbed by water (Jansen et al., 1994; Theisen-Kunde et al., 2011). With a 1/e penetration depth of only 80 μm, no direct laser radiation reached the cells covered by about 1.0 mm depth of culture medium with a total volume of 1200 μl. Thus cell warming is achieved by heat diffusion. Power-dependent medium temperature increase at the bottom level of the culture dish (about 1 mm depth of the culture medium) was calibrated by measuring the temperature with a fine thermocouple (200 μm diameter, HYP-0-33-1-T-G-60-SMPW-M, Omega® Engineering Inc., USA) every 100 ms. In order to know the temperature course and distribution at the cellular level, the tip of the thermocouple was inserted from the side of the culture dish through a water-tight micro hole to the dish bottom in a calibration setup without cells. The measurement was performed at the different radial positions of the dish bottom. The measured temperatures were evaluated by a LabVIEW program (National Instruments Corporation, Texas, USA) via an interface to a standard PC. The control of the laser irradiation was also performed on this program.

For the cell heating, culture medium was replaced by at 37 °C–prewarmed 1200 μl fresh medium shortly before irradiation, which was followed by the experimental procedure as shown in Fig. 2. Irradiation was performed with the pre-determined power-setups so that the peak temperature reaches around 40, 43, 46, 50, 58 °C at the center of culture dish bottom (2.7 W for 40 °C, 4.9 W for 43 °C, 7.7 W for 46 °C, 10.4 W for 50 °C, and 15.9 W for 58 °C). After irradiation, the culture dish was placed back to the incubator and kept until used for further examinations. An exemplary temperature curve is also presented in Fig. 2.

2.3. Cell viability test

At the time point of 3 and 24 h after laser irradiation, RPE cells were stained with ethidium homodimer III (EthD-III) for the detection of dead cells using a commercially available kit (Apoptotic/Necrotic/Healthy cells detection kit, PromoCell GmbH, Heidelberg, Germany). Briefly, the cells for the investigation were washed twice with binding buffer, and then the cells were incubated with EthD-III for 15 min at room temperature. After washing, the cells were fixed with 3.7% formaldehyde, which was then replaced by PBS, and observed under a fluorescence microscope with filters for excitation at 545–565 nm and for emission at 580–620 nm (Eclipse Ti, Nikon, Tokyo, Japan). In order to present the staining image of a whole culture, the images obtained with small magnification (×4) were stitched using specific imaging software of the microscope (NIS-Elements).

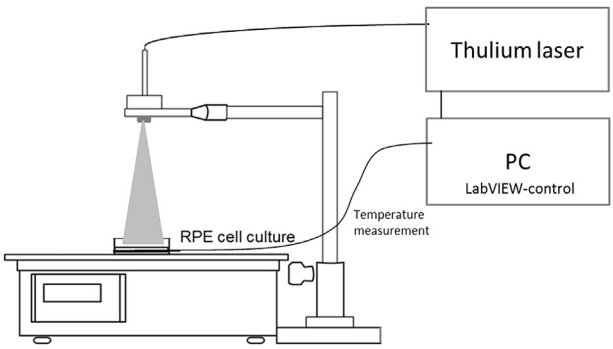

Fig. 1. A scheme of RPE cell culture irradiation setup with Thulium laser: The position of the laser probe was adjusted 12 cm above the RPE cell culture dish so that the irradiation spot diameter on the culture can be almost the same as the inner diameter of cell dish (30 mm). A LabVIEW software on the PC is connected to the laser irradiation system and controls the laser irradiation with the pre-set time schedules.

2.4. Oxidative stress by hydrogen peroxide (H_2O_2)

Twenty four hours after laser irradiation, the culture medium in some RPE cell cultures was replaced by 1.0 mM hydrogen peroxide (H_2O_2)–containing medium instead of the normal culture medium. After 5 h of H_2O_2 exposure, the conditioned mediums and the cells were separately collected for the measurement of the concentration of vascular endothelial growth factor (VEGF) in the medium and intracellular 4-HNE protein adducts, respectively.

2.5. Glutathione assay

Twenty four hours after laser irradiation, total glutathione, a sum of reduced glutathione (GSH) and oxidized glutathione (GSSG), was measured using Oxiselect Total Glutathione Assay Kit (Cell Biolabs, Inc, CA, USA). GSSG was assessed by adding 4-vinylpyridine (Sigma Aldrich, St. Louis, MO, USA) in each sample at the beginning of the assay in order to block the cycling reaction caused by GSH. The RPE cells were detached from the culture dish bottom by trypsinization 24 h after laser irradiation and washed with PBS twice. The cell pellet was then suspended in ice-cold 5% metaphosphoric acid (MPA) to achieve a cell concentration of 1×10^6 cells/ml. The cells were homogenized with TissueLyser LT (Qiagen GmbH, Hilden, Germany) and the suspensions were transferred to a microtube and centrifuged. The collected supernatant was analyzed for the assays. Assay for the total glutathione (GSH + GSSG) was conducted following manufacturer's introduction. For GSSG measurement, all samples and standards were incubated with 0.04 M 4-vinylpyridine for 1 h, and the further assay was conducted as in the total glutathione measurement. The amount of GSH was determined by subtracting the amount of GSSG by the amount of total glutathione.

2.6. 4-hydroxynonenal (4-HNE) assay

In order to investigate the influence of pre-hyperthermia on RPE cell response to the exogenously exposed oxidative stress in cultured RPE cells, one of the main endproducts of oxidative stress-induced lipid peroxidation, 4-hydroxynonenal (4-HNE), was measured using a commercially available kit (OxiSelect HNE-His Adduct ELISA Kit, Cell BIolabs, Inc., CA, USA). Briefly, the RPE cells were collected with cell scraper 5 h after the exposure to 1 mM H_2O_2, washed once and homogenized with TissueLyser LT. The suspensions were analyzed for the measurement of 4-HNE protein adduct, which was conducted as manufacturer's introduction. The measured amount of 4-HNE protein adduct was normalized with protein concentration measured with the bichinchoninic acid (BCA) method. Moreover, the dose-dependent effect of H_2O_2 on the amount of 4-HNE protein adduct in RPE cells was separately confirmed with different concentration of H_2O_2 (0, 0.5, and 1 mM).

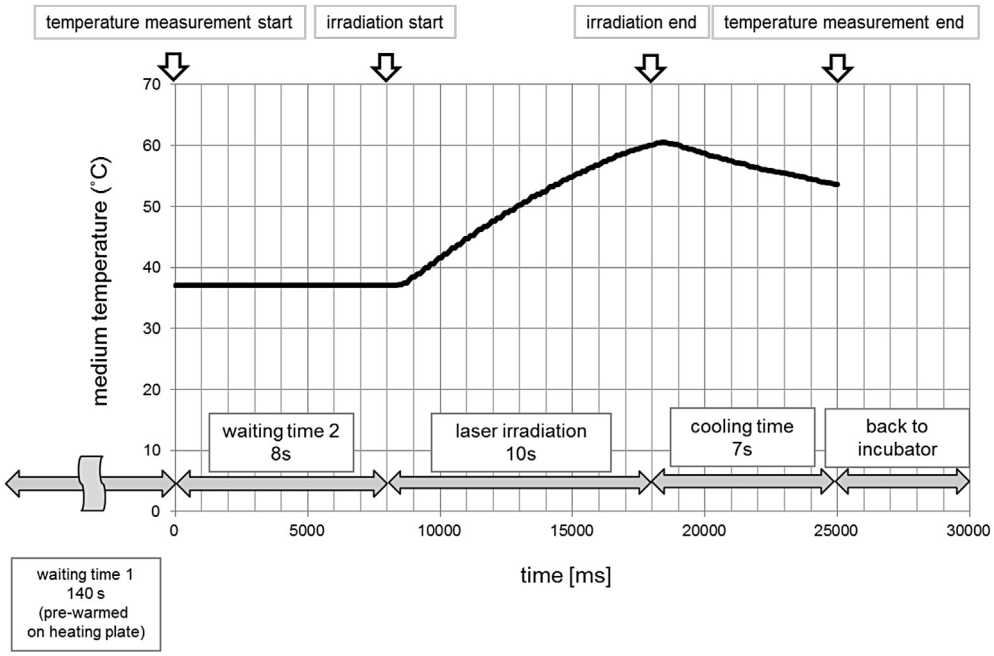

Fig. 2. A time sequence of the irradiation procedure and an exemplary temperature curve: Cell culture dish taken out from an incubator was placed on a heating plate (irradiation stage) for 148 s before irradiation in order to stabilize medium temperature around 37 °C. Irradiation took place for 10 s. The temperature rise at the cell level starts about a few hundreds milliseconds after the beginning of the irradiation, continues to increase until the end of irradiation, and decreases thereafter (also with a few hundreds milliseconds' delay). Seven seconds after the end of irradiation, the culture dish was placed back to the incubator (37 °C, 5% CO_2).

2.7. VEGF immunoassay

VEGF concentration in the conditioned culture medium was measured by Enzyme Linked Immunosorbent Assay (ELISA) using Quantikine ELISA assay kit (R&D systems, Minneapolis, MN, USA), according to the manufacturer's instructions. Conditioned mediums collected at the following time points were analyzed for VEGF concentration: 6 h after heat pre-treatment (total secretion in 6 h from the time point of heating), 24 h after heat treatment (total secretion in 24 h from the time point of heating), and 5 h after H_2O_2 exposure (total secretion in 5 h from the time point of H_2O_2 exposure; with or without pre-heating).

2.8. Statistics

Each experiment was conducted in triplicate, and the results are expressed as the mean ± standard deviation (SD). Statistical analyses were performed with Student's *t*-test and a two-sided *p*-value less than 0.05 was determined as significant.

3. Results

3.1. Temperature distribution following thulium laser irradiation at the cellular level

The temperature increase was proportional to the power, and the proportionality constant was determined to be 1.37 °C/W. In 10 second's irradiation, the peak temperature at the cellular level at the center of the spot (T_{max}) reached up to about 64 °C with the power range of the thulium laser used in this study. The measured peak temperature distribution in the culture dish at each power setting is presented in Fig. 3A. The two-dimensional temperature distribution at the cell level showed a bell-shaped curve, which fits to a Gaussian function according to the formula;

$$t(r) = t_{base} + A \cdot e^{\frac{-r^2}{2c^2}}$$

Where r stands for the distance from the center (cm), t_{base} is the temperature at the rim of the culture dish (°C), A is the amplitude, and c indicates the width of the curve. The parameters of fitted Gaussian curve for each T_{max} are shown in Fig. 3B.

3.2. Cell viability at 3 and 24 h after irradiation

Fig. 4A shows the representative images of a cell viability test with EthD-III 3 and 24 h after laser irradiation with $T_{max} = 50$ °C. Images were taken from more than 3 independent culture dishes for each temperature and time setting, and the diameter of EthD-III positive lesion was measured and the mean diameter (±SD) was calculated and shown in Fig. 4B. The EthD-III positive staining was not always round but sometimes elliptical form as shown in Fig. 4A, and in this case, the average of the longest and shortest diameter was calculated and used for the statistics. EthD-III has an affinity to the nucleic acids, but has no permeability through the cell membrane of living cells and cells under the process of apoptosis. Thus it can be used as a marker of dead cells. Its fluorescence property with the maximum emission/excitation at $\lambda = 530$nm/620 nm presents the dead cells in red fluorescence as is shown in Fig. 4A (24 h). The irradiation with $T_{max} \leq 50$ °C did not show apparent dead cells at the 3 h' time point. RPE cell cultures irradiated with $T_{max} \leq 46$ °C did not show apparent EthD-III positive staining until the 24 h' time point, while the cells irradiated with $T_{max} = 50$ °C, a very small lesion of EthD-III staining was detected in the center of the culture dish after 24 h with a diameter (d) = 0.35 ± 0.22 cm. Irradiation with $T_{max} = 58$ °C led to apparent dead lesion in the center of the culture dish already at the 3 h' time point ($d = 1.40 \pm 0.53$ cm), whose size appeared significantly larger at the 24 h' time point ($d = 1.76 \pm 0.65$ cm) (Fig. 4B).

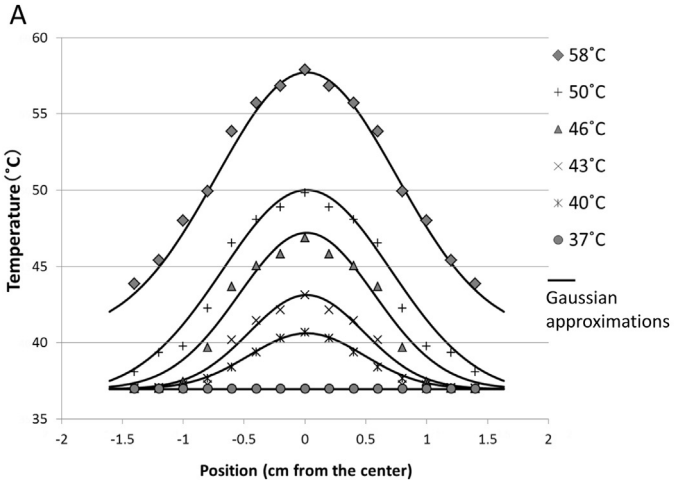

B

t_{max} (°C)	t_{base}	A	c
37	37.00	0	0
40	37.01	3.66	0.42
43	37.02	6.17	0.43
46	37.14	10.25	0.51
50	37.54	13.40	0.64
58	42.07	17.27	0.68

Fig. 3. Temperature profile in the cell culture (at the cellular level) for different power (=different T_{max}) settings: A) The lateral distributions of the peak temperature in a cell culture dish bottom following different irradiations are shown. The temperatures indicated beside the graph are the peak temperatures recorded at center of the dish (T_{max}). They show Gaussian-like distribution as in a typical retinal photocoagulation spot. B) The parameters for the Gaussian fit ($t(r) = t_{base} + A \cdot e^{-r^2/2c^2}$) for the irradiations with each T_{max} setting.

3.3. Determination of the threshold temperature for cell death after 3 and 24 h

The diameter measurement of EthD-III staining lesion as shown in Fig. 4 was conducted not only to visualize the effect of laser irradiation on cell viability, but also to determine the threshold temperature for cell death at the different time points after hyperthermia. By plotting the radius (diameter/2) of EhtD-III positive lesion (shown in Fig. 4B) in the graph of Fig. 2, the temperature at the rim of the EthD-III stained lesion, in other words, threshold temperature for cell death, was roughly determined; for the cell death at the early time point (3 h), where the cell death was detected only by the irradiation with T_{max} = 58 °C, the mean calculated threshold temperature was at 52.3 °C. For the threshold temperature for late cell death (not lethal at the 3 h' time point, but lethal at the 24 h' time point), the mean corresponding temperature at the rim of the lethal lesions of T_{max} = 50 °C and T_{max} = 58 °C was calculated at 50.3 °C and 50.8 °C, respectively.

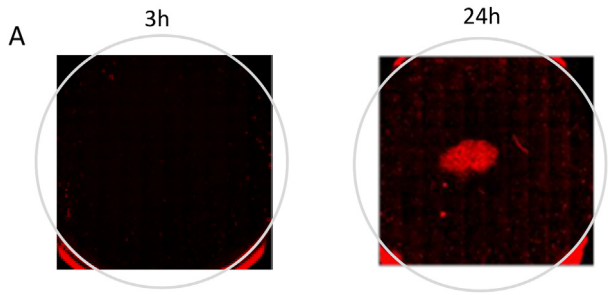

B

T_{max}	3h	24h
40°C	0	0
43°C	0	0
46°C	0	0
50°C	0	0.35 ± 0.22 cm
58°C	1.40 ± 0.53 cm	1.76 ± 0.65 cm

Fig. 4. Cell viability test with ethidium homodimer III (EthD-III) 3 and 24 h after thermal irradiation: A) Exemplary images of the culture dishes stained with EthD-III at the time point of 3 h (left) and 24 h (right) following the irradiation with T_{max} = 50 °C. The images were created by stitching of each fluorescence images examined with small magnification (×4) to present the image of whole culture dish. There is no apparent EthD-III staining (=dead cells) in RPE cell culture after 3 h (left), whereas the clear positive staining is observed in the center of the culture dish after 24 h (right). B) Mean diameters (±SD) of the EthD-III-positive area in RPE cell cultures irradiated with different T_{max} 3 and 24 h after irradiation are shown. The RPE cell culture irradiated with $T_{max} \leq 46$ °C did not show EthD-III positive area until 24 h after irradiation. Following the irradiation with T_{max} = 50 °C there was no EthD-III positive area in 3 h, whereas small EthD-III positive area was observed after 24 h. The irradiation with T_{max} = 58 °C induced apparent EthD-III positive area in the center of the culture, whose size was larger after 24 h. The diameter of the EthD-III positive area increased with T_{max} and with time.

3.4. Effect of hyperthermia on glutathione redox balance of RPE cells

Cells in a culture dish were collected after 24 h following laser irradiation with different T_{max} settings for the measurement of intracellular glutathione. Following sub-lethal irradiation with $T_{max} \leq 43$ °C, the concentration of reduced glutathione (GSH) was significantly increased compared to the RPE cells without hyperthermia (control: 37 °C), while following the irradiation with $T_{max} \geq 46$ °C the intracellular GSH level was significantly decreased, and this effect was increased with T_{max} (Fig. 5A). Oxidized glutathione (GSSG) was significantly reduced in the cells irradiated with T_{max} = 43 °C and 46 °C, while it was significantly increased at the higher T_{max} (Fig. 5B). The ratio of GSH/GSSG was the highest in the cells irradiated with T_{max} = 43 °C ($p < 0.01$), whereas T_{max} = 41 °C and 46 °C did not change the ratio. The lethal irradiations at $T_{max} \geq 50$ °C significantly reduced the GSH/GSSG ratio (Fig. 5C).

3.5. Effect of pre-hyperthermia on H_2O_2-induced 4-HNE formation

Twenty four hours after the irradiation (pre-hyperthermia) with different T_{max}, oxidative stress was challenged to the RPE cells by exposing the cells to 1 mM H_2O_2 for 5 h. Intracellular oxidative stress status was assessed by measuring 4-HNE. Only pre-irradiation (T_{max} from 40 to 58 °C) did not show significant change of 4-HNE level in 24 h (data not shown). The dose-dependent effect of H_2O_2 on 4-HNE generation in RPE cells was confirmed, where $H_2O_2 \geq 0.5$ mM was shown to induce significant increase of 4HNE adduct in RPE cells (Fig. 6A). The H_2O_2 (1 mM)-induced formation of 4-HNE adduct was significantly lower in the

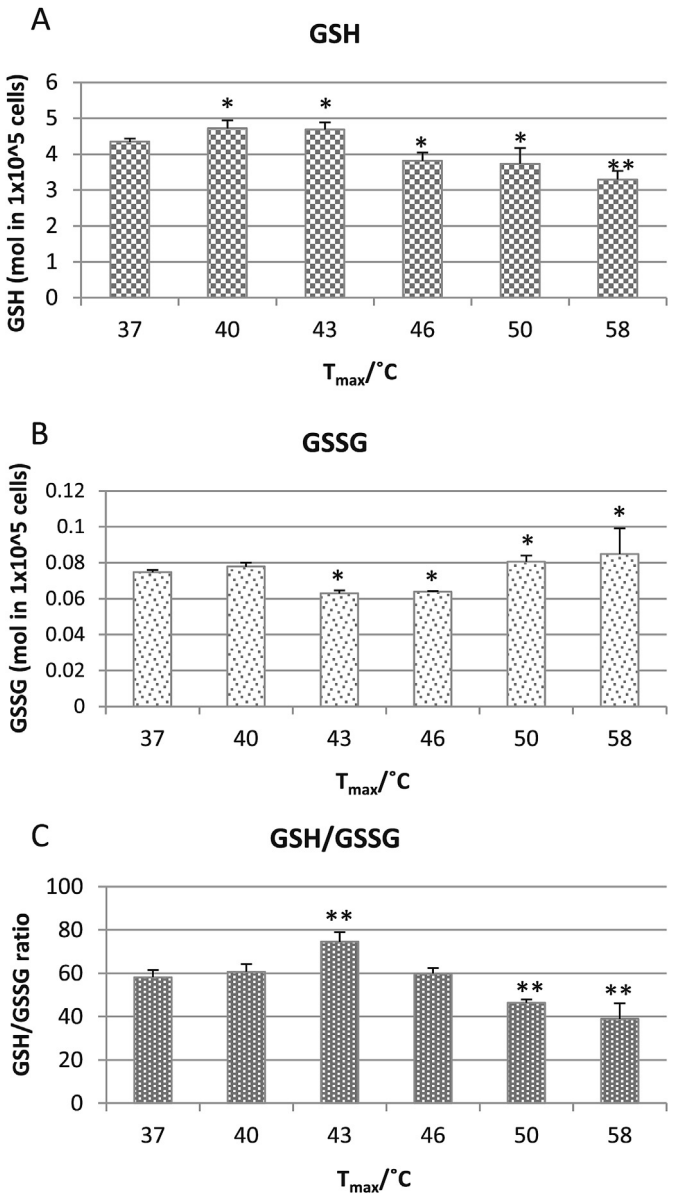

Fig. 5. Glutathione (GSH, GSSG) and the GSH/GSSG ratio in RPE cells 24 h after thermal laser irradiation with different T_{max}: A) intracellular GSH after irradiations with different T_{max}. The irradiation with $T_{max} = 40$ °C and 43 °C increased intracellular GSH significantly. On the other hand, the irradiation with $T_{max} \geq 50$ °C significantly decreased it. B) Intracellular GSSG after the irradiation with different $T_{max.}$ The irradiation with $T_{max} = 43$ °C and 46 °C significantly decreased GSSG, whereas the irradiation with $T_{max} \geq 50$ °C significantly increases it. C) GSH/GSSG ratio. The irradiation with $T_{max} = 43$ °C is resulted in the significant increase of GSH/GSSG ratio (74.6) from the non-treated control (58.2). The irradiation with $T_{max} \geq 50$ °C significantly decreased the ratio. ($^{*}p < 0.05$, $^{**}p < 0.01$ compared to non-treated control (37 °C)).

RPE cells irradiated with $T_{max} = 43$ °C ($p < 0.05$) compared to non-pretreated control cells, whereas in the cells with lethal irradiation $T_{max} \geq 50$ °C the H_2O_2-induced of 4-HNE was significantly higher ($p < 0.05$) (Fig. 6B).

3.6. Effect of hyperthermia and oxidative stress on VEGF secretion from RPE cells

VEGF secretion into the conditioned medium of RPE cell cultures during 6 h and 24 h following laser irradiation was measured and the results are shown in Fig. 7A and B, respectively. In the first 6 h, the tendency was shown that sub-lethal hyperthermia with $T_{max} \leq 46$ °C induced the increase of VEGF secretion temperature-dependently, although only the irradiation with $T_{max} = 46$ °C resulted in the significant increase of VEGF secretion (114.9 ± 2.0%, $p < 0.05$) compared to non-irradiated control cells (37 °C) (Fig. 7A). Sum of VEGF secretion in 24 h following laser irradiation did not show any significant difference among the different temperature settings (Fig. 7B).

Five hour-long exposure of 1 mM H_2O_2 induced a significant increase of VEGF concentration in the conditioned medium of the RPE cell culture without pre-hyperthermia (125.8%, $p < 0.01$, Fig. 7C). The VEGF secretion in 5 h following H_2O_2 exposure was significantly reduced in the cultures previously irradiated sub-lethally with $T_{max} = 40$, 43, and 46 °C (87.0%, 69.5%, and 91.0%, respectively) compared to the non-irradiated control (37 °C), where, most notably, the irradiation with $T_{max} = 43$ °C led to the lowest secretion of VEGF after H_2O_2 exposure (Fig. 7C).

4. Discussion

Despite that retinal photocoagulation is one of the most common and successful laser therapies in medicine, the viability and functionality of RPE cells after irradiation, especially temperature-dependent cell responses, have been still very little studied. For the purpose of the study on the effect of hyperthermia on RPE cell cultures, some experimental approaches have been attempted by researchers (Denton et al., 2006, 2009; Cordeiro et al., 2010; Klettner et al., 2012). Some of the studies utilized a heating plate with pre-warmed medium or incubators to warm the cells, which requires a relatively long time, at least minutes long, to reach a stable aimed temperature. Another limitation of using heating plates is the difference between the setting temperature of the heating plate and the real temperature at the cellular level in the culture dish bottom. It is caused by heat diffusion through the plastic dish bottom (about 1 mm thickness) and the medium (typically a few millimeters height) owing to the temperature difference between the heating plate and the surrounding air. Thus, with these methods a quick temperature increase with precise temperature and time control is almost impossible. In a typical laser spots in retinal photocoagulation or in TTT, a Gaussian-like temperature distribution develops within ms to seconds, with the highest temperature in the center of the spot at the level of the RPE (Kandula et al., 2006; Brinkmann et al., 2012). Thus, it is to note that the total response of the RPE to a thermal laser irradiation is a sum of the response from the number of cells times its certain temperature; a mixture of the responses from cells at high temperature in the center and cells at lower temperature at a certain distance from the center. Moreover, considering a single laser temperature profile, the number of the cells irradiated with the lower temperature is much more than the number of cells with higher temperature. Therefore, we aimed to establish a system which enables a quick temperature rise and a similar temperature distribution as in clinical thermal laser. In order to obtain a significant temperature rise in a short period of time, high power laser irradiation is an appropriate method. Furthermore, in order to obtain a higher amount of expressed genes or proteins, we chose a large area irradiation in cell culture dish (30 mm), which improves the accessibility of studying thermal laser-induced cell biochemical responses with an in-vitro model.

The most laser sources used for retinal treatment have a wavelength, which is well absorbed by the RPE's melanosomes, typically in the green or yellow spectral range. However, for RPE cell culture experiment this wavelength range is not suitable due to the variability of RPE pigmentation and the decreasing pigmentation through culture passaging. As artificial absorbers, isolated

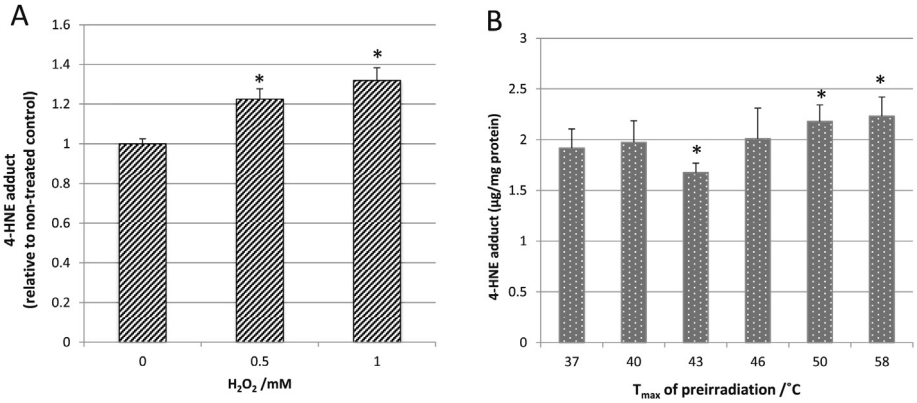

Fig. 6. Effect of H_2O_2 exposure on the formation of intracellular 4-HNE protein adduct in RPE cells: A) Effect of H_2O_2 (0, 0.5, 1 mM, for 5 h) on the amount of 4-HNE protein adduct in RPE cells. H_2O_2 induced the significant increase of intracellular 4-HNE protein adduct in RPE cells dose-dependently. B) 4-HNE protein adduct in RPE cells after 5 h-exposure to 1 mM H_2O_2 following different thermal preirradiations performed 24 h prior to the H_2O_2 exposure. Intracellular concentration of 4-HNE protein adduct was significantly lower in the RPE cells which were previously irradiated with $T_{max} = 43$ °C compared to the cells without preirradiation (37 °C). On the other hand, the RPE cell cultures irradiated with $T_{max} \geq 50$ °C showed the significantly higher amount of 4-HNE protein adducts. ($^*p < 0.05$ compared to non-treated control; 0 mM H_2O_2 in (A) and 37 °C in (B)).

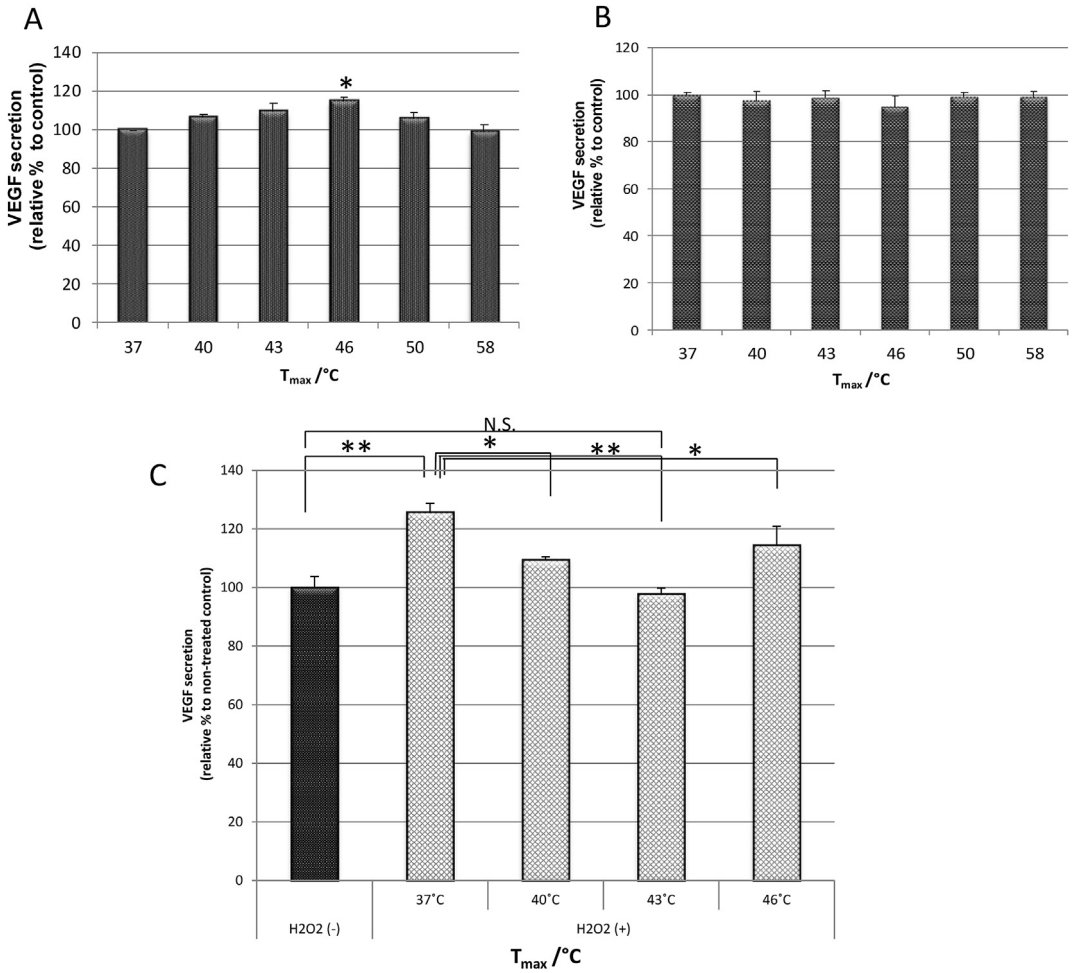

Fig. 7. VEGF secretion from RPE cells in 6 h and 24 h following irradiation (A, B) and the effect of preirradiations on H_2O_2-induced VEGF secretion from RPE cells (C): A) VEGF concentration in the conditioned medium of RPE cell culture collected after 6 h following laser irradiation. The results are presented as the relative ratio to the non-irradiated control (37 °C). The irradiation with $T_{max} \leq 46$ °C slightly increased VEGF secretion from RPE cells seemingly in a temperature-dependent manner, where the significance was seen at the irradiation with $T_{max} = 46$ °C. The lethal irradiation with $T_{max} \geq 50$ °C did not increase total amount of VEGF secretion in 6 h following irradiation. B) There were no significant differences in total amount of VEGF secretion in 24 h between the laser irradiated cultures with any T_{max} and non-treated control (37 °C). C) The effect of sub-lethal thermal preirradiation on H_2O_2-induced VEGF secretion from RPE cells. The VEGF in the conditioned medium from 5 h (=during H_2O_2 exposure) was collected and VEGF concentration was measured. In non-irradiated RPE cell culture (37 °C), 1 mM H_2O_2 induced a significant increase of VEGF secretion (125.7%), whereas in sub-lethally preirradiated ($T_{max} \leq 46$ °C) cultures secreted significantly lower amount of VEGF during H_2O_2 exposure. ($^*p < 0.05$, $^{**}p < 0.01$).

melanosomes (Denton et al., 2009, 2006; Shrestha et al., 2011) or black paper beneath the dish bottom (Yoshimura et al., 1995) were previously reported. However, these methods still have a limitation in realizing a Gaussian-like temperature due to hot spots at strong absorbers, and thus are considered to be unsuitable to investigate accurate temperature-dependent cell responses. In order to enable heating independent of cellular pigmentation a laser with appropriate power for fast heating and a wavelength strongly absorbed by the culture medium is demanded. A good candidate is the Thulium-laser with a wavelength of 1.94 μm, which is strongly absorbed by water (Maher, 1979). The penetration depth – the depth until 63% of the energy is absorbed - of the laser radiation in culture medium is around 80 μm. Thus the temperature increase at the cellular level, which is covered by about 1.0 mm culture medium, is all led by thermal diffusion. This causes the slight delay (a few hundred milliseconds) of the beginning of temperature increase at the cellular level, as shown in the graph of Fig. 2. The power-temperature calibration data show the proportional relation between the laser power and the temperature increase (1.37 °C/W after 10 s), with a high repeatability. Although the absorbers are different between the usage of 532 nm laser and 1900 nm laser, directly and indirectly by cells, respectively, the temperature distribution at the cellular level is Gaussian-like in both cases. Moreover, the temporal temperature course during irradiation is also similar to the temperature course measured with an optoacoustic technique in in-vivo measurement (Brinkmann et al., 2012). In total, therefore, this thulium laser irradiation system seems to be a useful experimental setup for the cell culture research to investigate temperature-resolved cellular responses. Further shortening of the irradiation time is also possible by using a Thulium laser with higher power, up to 150 W continuous wave are commercially available (IPG Photonics Corp, MA, USA).

Denton et al. presented previously a novel method to measure the temperature increase during 514 nm Argon laser irradiation on cultured RPE cells using a fast infrared camera (Denton et al., 2009, 2011). The big advantage of their method is the acquaintance of temperature information with high temporal and spatial resolution, which is able to be referred to the cell viability test performed afterward. They used human RPE cell line with phagocytized melanosomes as light absorbers, and thus the damage extent is not as constant as in our setup due to the wide range of absorption differences. Therefore, their method is very useful for the investigation of the damage thresholds, but might be less suitable for the study that requires a repeatable temperature increase, e.g. for temperature-dependent protein expression.

In the current study, RPE cell viability following laser-induced hyperthermia was investigated over time until 24 h after irradiation. The results of the viability test with EthD-III presented that the temperature threshold for RPE cells death with our irradiation setup ($t = 10$ s) in 3 h might be at $T_{max} \approx 52$ °C, and in 24 h at $T_{max} \approx 50$ °C. The fluorescence probe EthD-III is a highly positively charged nucleic acid probe, which is permeant to the necrotic and dead cells, and is fluorescent at $\lambda_{ex}/\lambda_{em} = 580/620$ nm. Thus in this method, we did not distinguish the dead cells either through apoptotic or necrotic pathways, which has to be further investigated, in order to elucidate cell death mechanisms by lethal hyperthermia in more detail. The previous studies presented the RPE cell viability following laser irradiation mostly at single time point (Denton et al., 2009; Sramek et al., 2011a), however, present study clearly suggests that significant amount of late cell death takes place following thermal irradiation, which is not detected after 3 h but apparently appeared after 24 h. This phenomenon has to be taken into account in discussing threshold temperatures for cell death. The mechanisms of the temperature increase-induced immediate/late cell death are to be further elucidated.

There are some evidences from in-vitro and in-vivo studies, suggesting that sub-lethal hyperthermia on RPE cell may induce alterations of RPE cell function (Cordeiro et al., 2010; Sekiyama et al., 2011). An in-vivo study by Sekiyama et al. (2011) suggests the therapeutic efficacy of sub-lethal hyperthermia on the RPE by reducing choroidal neovascularization through the increasing expression of antiangiogenic factors. An in-vivo study by Sramek et al. (2011a) examined the dynamic temperature threshold of heat shock protein 70 (HSP70) expression by sub-lethal laser irradiation on mouse, and suggested the therapeutic possibility of non-damaging retinal phototherapy. Moreover, recent clinical studies reported the therapeutic benefit of TTT. A low-dose TTT in combination with intravitreous bevacizumab (Schöderberg et al., 2012) or TTT with sub-Tenon's injection of triamcinolone acetonide (Agnieszka, 2010), showed significant benefits in the treatment of neovascular AMD. Therefore, the study to elucidate therapeutic mechanisms of mild temperature increase of RPE cells as the current study is considered to be of great importance.

In recent years, numerous studies have suggested that increasing oxidative stress, as lipid peroxidation, and protein or DNA oxidation, plays a significant role in the degenerative alterations of aged organisms (Chakraborty et al., 2013; Magenta et al., 2013; Cencioni et al., 2013). In particular, lipid peroxidation around the RPE has been shown to play a critical role in the pathogenesis of AMD (Nowak,2013; Kauppinen et al., 2012), and to be associated with different pathological changes of RPE cells, such as cell viability (Qin and Rodrigues, 2010), apoptotic change (Sharma et al., 2008), and lipofscinogenesis (Krohne et al., 2010b). Increase of cellular oxidative stress can be caused not only by the increase of oxidants, but also by the decrease of cellular anti-oxidant defense system. The goal of this study was to investigate the possibility of improving cellular anti-oxidant defense potential of RPE cells by sub-lethal laser irradiation.

Hyperthermia may induce cellular oxidative stress and can damage multiple cell components resulting in cell death (Lin et al., 1991; Kikusato and Toyomizu, 2013). However, when the cells are exposed to certain amount of stresses below the damage threshold, it may strengthen their cell defense system, which is called adaptive response (Crawford and Davies, 1994; Jeggo et al., 1977). A previous report presented the cell adaptive responses in Chinese hamster fibroblasts against H_2O_2-induced cell damage through pretreatment of low dose of H_2O_2 or sub-lethal heat shock (Spitz et al., 1987). Oka et al. (2013) showed that heat-shock pretreatment reduces liver injury and aids liver recovery after partial hepatectomy in mice. In the current study, we could present the acquisition of some resistance against H_2O_2 in RPE cells through sub-lethal hyperthermia pre-treatment, which suggests that the hyperthermic and H_2O_2-induced stresses may be mediated by similar signal cascades. Mild hyperthermia may also induce cellular alterations such as ROS formation (Pallepati and Averill-Bates, 2011), secretion of VEGF (Klettner et al., 2012), and activation of stress-response transcription factors as NF-kB (Nivon et al., 2009). Molecular chaperones, heat shock proteins, such as HSP 70 and HSP 90, are induced to protect the cells from protein misfolding or apoptotic cell death (Bettaieb and Averill-Bates, 2005), whose induction are suggested to be an adaptive response caused by the mild increase of ROS generation through hyperthermia (Pallepati and Averill-Bates, 2011).

GSH is a major antioxidant in many mammalian cells (Meister, 1994; Meister and Anderson, 1983). Reduction of the generated ROS by GSH causes the decrease of GSH and increase of GSSG in cells, which will be recycled to GSH with the simultaneous oxidation of nicotinamide adenine dinucleotide phosphate (NADPH). When cells are exposed to increased levels of oxidative stress, GSSG will accumulate and the ratio of GSH to GSSG will decrease.

Therefore, the GSH/GSSG ratio is a useful indicator of cellular oxidative stress status and can be used to monitor the cellular antioxidant potential. Previous studies have suggested the endogenous GSH has a protective effect of RPE from oxidative injury (Sternberg et al 1993). Regarding heat-induced alteration of intracellular glutathione, Pallepati P et al. reported that mild hyperthermia (40 °C for 3 h) on HeLa cells increased intracellular total glutathione and other defense proteins, such as antioxidant proteins and anti-apoptotic proteins (Pallepati and Averill-Bates, 2011). On the other hand, Zhang et al. (2003) reported the significant decrease of GSH/GSSG ratio in the liver tissue by heating the rat twice to 41 °C for 30 min. To our best knowledge, alteration of GSH/GSSG ratio in RPE cells following sub-lethal hyperthermia with different temperature settings had not been investigated yet to date. Our results could present the temperature-dependent difference in intracellular glutathione level in RPE cells and showed that the irradiation with $T_{max} = 43$ °C could lead to the highest GSH/GSSG ratio at the time point of 24 h after irradiation, whereas the irradiation with $T_{max} = 46$ °C did not change the ratio and rather decreased the amount of GSH. These results suggest that laser-induced sub-lethal hyperthermia on RPE cell may modify cellular antioxidant property under precise temperature- and time- controls for irradiation.

This positive modification of cellular antioxidant property characterized by GSH/GSSG ratio induced by just 10-s-long irradiation was further proven in the following experiments with H_2O_2 exposure in the current study. The RPE cells which were pre-irradiated with $T_{max} = 43$ °C showed the lowest amount of H_2O_2-induced 4-HNE adducts. It is strongly assumed to be owing to the highest amount of GSH and the highest GSH/GSSG ratio induced by the irradiation, since H_2O_2 may be directly reduced by GSH ($H_2O_2 + 2GSH \rightarrow 2H_2O + GSSG$, catalyzed by glutathione peroxidase). Moreover, previous reports have presented that GSH forms the conjugate with 4-HNE via glutathione S-transferases (GSTs) and it plays a significant role in the detoxification of endogenously generated toxic 4-HNE (Singhal et al., 1995; Spitz et al., 1991). In the current study, we did not measure the expression of GSTs, and thus the contribution of the detoxification function of GSH via GSTs in this study is still not clear, which has to be further investigated.

In the physiological conditions, cultured RPE cells produce considerable quantities of VEGF as a basic secretion (Adamis et al., 1993; Ikeda et al., 2006; Miura et al., 2010; Klettner et al., 2013). Hyperthermia induced-VEGF secretion from cultured RPE has been reported previously (Klettner et al., 2012; Miura et al., 2009). In our study, too, the 10-s-long irradiation also induced temperature-dependent increase of VEGF secretion in the first 6 h following sub-lethal irradiation, in which a significant increase was seen at $T_{max} = 46$ °C. Following the lethal irradiation, as following $T_{max} = 50$ °C and $T_{max} = 58$ °C, the accumulated VEGF secretion in 6 h is not significantly increased, and this is considered to be due to the decreased amount of living RPE cells. After 24 h, these differences were not detected any more, but interestingly, oxidative stress-induced VEGF secretion from RPE cells showed a significant difference dependent on the way of pre-hyperthermia treatment. The sub-lethal hyperthermia preirradiation, in particular, with $T_{max} = 43$ °C, led to the significantly lower amount of oxidative stress-induced VEGF secretion than the RPE cells without pre-irradiation. As one of the mechanisms, it is considered due to the high amount of GSH and GSH/GSSG ratio, which may inhibit exogenous H_2O_2 from activating the signal cascades, as MAPK (Klettner et al., 2013) or VEGF-R2/PI3K/Akt Pathway (Byeon et al., 2010), which were shown to lead to the increased VEGF expression in RPE cells. These results suggest that the sub-lethal hyperthermia may induce RPE cell adaptive response, resulting in the suppression of oxidative stress-induced VEGF secretion. Moreover, it is also conceivable that hyperthermia-induced slight increase of VEGF might be requisite for cellular adaptive response, and thus continuous neutralization of VEGF in the patients with AMD or macular edema might affect RPE cell adaptive response, and eventually RPE cell survival. The previous report by Byeon et al. (2010) suggesting that VEGF might be an autocrine survival factor for RPE cells under oxidative stress, supports this hypothesis.

The results concerning RPE cell biochemical responses shown in the current study are the cumulative effect from cells over the whole culture dish exposed to a wide range of temperature rise with a spatially Gaussian-like distribution and temporally a logarithmically rising and falling course. This is comparable to the clinical practice with a similar temperature course during retinal thermal therapies. Thus we consider that our method reflects the realistic RPE responses following retinal laser irradiation. However, for the sake of best understanding, it would be desirable to expose all cells with a constant uniform spatial and temporal temperature rise. Unfortunately, owing to heat flux dynamics, this goal is impossible to achieve, but may, however, be approached: Temporally, a power controlled heating with a fast high power heating quickly providing the desired temperature rise, followed by a reduced power to keep the desired temperature would be a step forward to achieve this goal. For quick cooling, a high power Peltier cooler most close to the cells might be used. Spatially, a laser beam profile modulation for heating, starting with a top hat profile and ending up with a donut profile may be implemented. Sramek et al. has already proposed and developed a ring-shaped beam in order to improve retinal photocoagulation towards a more uniform temperature distribution (Sramek et al., 2011b).

In summary, we introduced a novel in-vitro irradiation setup, which may create a single laser spot on RPE cell culture with a temperature distribution as is expected to take place in clinical treatment, and enables to irradiate RPE cell culture with precise temperature/time control with high repeatability. Moreover, using this setup, we could present the sub-lethal irradiation-induced increase of intracellular antioxidant in RPE cells, along with the inhibited amount of oxidative stress-induced lipid peroxidation endproduct and VEGF secretion upon accurately measured temperature increase. Further investigation is necessary for better understanding of therapeutic mechanisms of sub-lethal RPE thermal laser treatment, and to find new therapeutic possibilities using sub-lethal cell hyperthermia within a specific temperature/time window.

Acknowledgment

Authors would like to thank Veit Danicke for his technical support. This study was supported by German federal ministry of education and research (BMBF), grant #. 01EZ0733.

References

Adamis, A.P., Shima, D.T., Yeo, K.T., Yeo, T.K., Brown, L.F., Berse, B., D'Amore, P.A., Folkman, J., 1993. Synthesis and secretion of vascular permeability factor/vascular endothelial growth factor by human retinal pigment epithelial cells. Biochem. Biophys. Res. Commun. 193, 631–638.

Agnieszka, K.T., 2010. Transpupillary thermotherapy (TTT) with injections of triamcinolone acetonide under posterior Tenon's capsule in the treatment of exudative age-related macular degeneration (AMD). Klin. Ocz. 112, 289–292.

Avery, R.L., Pieramici, D.J., Rabena, M.D., Castellarin, A.A., Nasir, M.A., Giust, M.J., 2006. Intravitreal bevacizumab (Avastin) for neovascular age-related macular degeneration. Ophthalmology 113, 363–372.

Bailey, T.A., Kanuga, N., Romero, I.A., Greenwood, J., Luthert, P.J., Cheetham, M.E., 2004. Oxidative stress affects the junctional integrity of retinal pigment epithelial cells. Invest. Ophthalmol. Vis. Sci. 45, 675–684.

Beatty, S., Koh, H., Phil, M., Henson, D., Boulton, M., 2000. The role of oxidative stress in the pathogenesis of age-related macular degeneration. Surv. Ophthalmol. 45, 115–134.

Bettaieb, A., Averill-Bates, D.A., 2005. Thermotolerance induced at a mild temperature of 40 degrees C protects cells against heat shock-induced apoptosis. J. Cell. Physiol. 205, 47–57.

Brambilla, G., Sciabà, L., Faggin, P., Maura, A., Marinari, U.M., Ferro, M., Esterbauer, H., 1986. Cytotoxicity, DNA fragmentation and sister-chromatid exchange in Chinese hamster ovary cells exposed to the lipid peroxidation product 4-hydroxynonenal and homologous aldehydes. Mutat. Res. 171, 169–176.

Brinkmann, R., Koinzer, S., Schlott, K., Ptaszynski, L., Bever, M., Baade, A., Luft, S., Miura, Y., Roider, J., Birngruber, R., 2012. Real-time temperature determination during retinal photocoagulation on patients. J. Biomed. Opt. 17, 061219.

Byeon, S.H., Lee, S.C., Choi, S.H., Lee, H.K., Lee, J.H., Chu, Y.K., Kwon, O.W., 2010. Vascular endothelial growth factor as an autocrine survival factor for retinal pigment epithelial cells under oxidative stress via the VEGF-R2/PI3K/Akt. Invest. Ophthalmol. Vis. Sci. 51, 1190–1197.

Cai, J., Nelson, K.C., Wu, M., Sternberg Jr., P., Jones, D.P., 2000. Oxidative damage and protection of the RPE. Prog. Retin. Eye. Res. 19, 205–221.

Cencioni, C., Spallotta, F., Martelli, F., Valente, S., Mai, A., Zeiher, A.M., Gaetano, C., 2013. Oxidative stress and epigenetic regulation in ageing and age-related diseases. Int. J. Mol. Sci. 14, 17643–17663.

Chakraborty, S., Bornhorst, J., Nguyen, T.T., Aschner, M., 2013. Oxidative stress mechanisms underlying Parkinson's disease-associated neurodegeneration in *C. elegans*. Int. J. Mol. Sci. 14, 23103–23128.

Chen, H., Liu, B., Lukas, T.J., Neufeld, A.H., 2008. The aged retinal pigment epithelium/choroid: a potential substratum for the pathogenesis of age-related macular degeneration. PLoS One 3, e2339.

Cordeiro, S., Seyler, S., Stindl, J., Milenkovic, V.M., Strauss, O., 2010. Heat-sensitive TRPV channels in retinal pigment epithelial cells: regulation of VEGF-A secretion. Invest. Ophthalmol. Vis. Sci. 51, 6001–6008.

Crawford, D.R., Davies, K.J., 1994. Adaptive response and oxidative stress. Environ. Health. Perspect. 102 (Suppl. 10), 25–28.

Davies, S., Elliott, M.H., Floor, E., Truscott, T.G., Zareba, M., Sarna, T., Shamsi, F.A., Boulton, M.E., 2001. Photocytotoxicity of lipofuscin in human retinal pigment epithelial cells. Free. Radic. Biol. Med. 31, 256–265.

Denton, M.L., Foltz, M.S., Estlack, L.E., Stolarski, D.J., Noojin, G.D., Thomas, R.J., Eikum, D., Rockwell, B.A., 2006. Damage thresholds for exposure to NIR and blue lasers in an in vitro RPE cell system. Invest. Ophthalmol. Vis. Sci. 47, 3065–3073.

Denton, M.L., Foltz, M.S., Noojin, G.D., Estlack, L.E., Thomas, R.J., Rockwell, B.A., 2009. Determination of threshold average temperature for cell death in an in vitro retinal model using thermography. Proc. SPIE, 71750G.

Denton, M.L., Noojin, G.D., Foltz, M.S., Clark 3rd, C.D., Estlack, L.E., Rockwell, B.A., Thomas, R.J., 2011. Spatially correlated microthermography maps threshold temperature in laser-induced damage. J. Biomed. Opt. 16, 036003.

Esterbauer, H., Schaur, R.J., Zollner, H., 1991. Chemistry and biochemistry of 4-hydroxynonenal, malonaldehyde and related aldehydes. Free. Radic. Biol. Med. 11, 81–128.

Gitter, K.A., Cohen, G., Baber, B.W., 1975. Photocoagulation in venous occlusive disease. Am. J. Ophthalmol. 79, 578–581.

Havener, W.H., 1964. Technical Aspects of laser coagulation. Am. J. Ophthalmol. 58, 38–41.

Ikeda, Y., Yonemitsu, Y., Onimaru, M., Nakano, T., Miyazaki, M., Kohno, R., Nakagawa, K., Ueno, A., Sueishi, K., Ishibashi, T., 2006. The regulation of vascular endothelial growth factors (VEGF-A, -C, and -D) expression in the retinal pigment epithelium. Exp. Eye. Res. 83, 1031–1040.

Jansen, E.D., van Leeuwen, T.G., Motamedi, M., Borst, C., Welch, A.J., 1994. Temperature dependence of the absorption coefficient of water for midinfrared laser radiation. Lasers. Surg. Med. 14, 258–268.

Jeggo, P., Defais, T.M., Samson, L., Schendel, P., 1977. An adaptive response of *E. coli* to low levels of alkylating agent: comparison with previously characterised DNA repair pathways. MGG – Mol. General. Genet. 157, 1–9.

Kaemmerer, E., Schutt, F., Krohne, T.U., Holz, F.G., Kopitz, J., 2007. Effects of lipid peroxidation-related protein modifications on RPE lysosomal functions and POS phagocytosis. Invest. Ophthalmol. Vis. Sci. 48, 1342–1347.

Kandulla, J., Elsner, H., Birngruber, R., Brinkmann, R., 2006. Noninvasive optoacoustic online retinal temperature determination during continuous-wave laser irradiation. J. Biomed. Opt. 11, 041111.

Kauppinen, A., Niskanen, H., Suuronen, T., Kinnunen, K., Salminen, A., Kaarniranta, K., 2012. Oxidative stress activates NLRP3 inflammasomes in ARPE-19 cells–implications for age-related macular degeneration (AMD). Immunol. Lett. 147, 29–33.

Kikusato, M., Toyomizu, M., 2013. Crucial role of membrane potential in heat stress-induced overproduction of reactive oxygen species in avian skeletal muscle mitochondria. PLoS One 8, e64412.

Klettner, A., Faby, H., Hillenkamp, J., Roider, J., 2012. Temperature-dependent vascular endothelial growth factor (VEGF) induction in human retinal pigment epithelium – implications for transpupillary thermotherapy in uveal melanoma. Acta. Ophthalmol. 90 (Suppl. 249), 0.

Klettner, A., Westhues, D., Lassen, J., Bartsch, S., Roider, J., 2013. Regulation of constitutive vascular endothelial growth factor secretion in retinal pigment epithelium/choroid organ cultures: p38, nuclear factor κB, and the vascular endothelial growth factor receptor-2/phosphatidylinositol 3 kinase pathway. Mol. Vis. 19, 281–291.

Koinzer, S., Schlott, K., Ptaszynski, L., Bever, M., Kleemann, S., Saeger, M., Baade, A., Caliebe, A., Miura, Y., Birngruber, R., Brinkmann, R., Roider, J., 2012. Temperature-controlled retinal photocoagulation–a step toward automated laser treatment. Invest. Ophthalmol. Vis. Sci. 53, 3605–3614.

Kosower, N.S., Kosower, E.M., 1978. The glutathione statue of the cell. Int. Rev. Cytol. 54, 109–160.

Krohne, T.U., Kaemmerer, E., Holz, F.G., Kopitz, J., 2010a. Lipid peroxidation products reduce lysosomal protease activities in human retinal pigment epithelial cells via two different mechanisms of action. Exp. Eye. Res. 90, 261–266.

Krohne, T.U., Stratmann, N.K., Kopitz, J., Holz, F.G., 2010b. Effects of lipid peroxidation products on lipofuscinogenesis and autophagy in human retinal pigment epithelial cells. Exp. Eye. Res. 90, 465–471.

Lin, P.S., Quamo, S., Ho, K.C., Gladding, J., 1991. Hyperthermia enhances the cytotoxic effects of reactive oxygen species to Chinese hamster cells and bovine endothelial cells in vitro. Radiat. Res. 126, 43–51.

Magenta, A., Greco, S., Gaetano, C., Martelli, F., 2013. Oxidative stress and MicroRNAs in vascular diseases. Int. J. Mol. Sci. 14, 17319–17346.

Maher, E.F., 1979. Transmission and Absorption Coefficients for Ocular Media of the Rhesus Monkey. USAF School of Aerospace Medicine.

Mainster, M.A., Reichel, E., 2000. Transpupillary thermotherapy for age-related macular degeneration: long-pulse photocoagulation, apoptosis, and heat shock proteins. Ophthalmic Surg Lasers 31, 359–373.

Meister, A., 1994. Glutathione, ascorbate, and cellular protection. Cancer. Res. 54, 1969s–1975s.

Meister, A., Anderson, M.E., 1983. Glutathione. Annu. Rev. Biochem 52, 711–760 (Review).

Mettu, P.S., Wielgus, A.R., Ong, S.S., Cousins, S.W., 2012. Retinal pigment epithelium response to oxidant injury in the pathogenesis of early age-related macular degeneration. Mol. Asp. Med. 33, 376–398.

Meyer-Schwickerath, G., 1954. Light coagulation: a method for treatment and prevention of the retinal detachment. Albr. Von. Graefes. Arch. Ophthalmol. 156, 2–34.

Ming, Y., Algvere, P.V., Odergren, A., Berglin, L., van der Ploeg, I., Seregard, S., Kvanta, A., 2004. Subthreshold transpupillary thermotherapy reduces experimental choroidal neovascularization in the mouse without collateral damage to the neural retina. Invest. Ophthalmol. Vis. Sci. 45, 1969–1974.

Miura, Y., Klettner, A., Noelle, B., Hasselbach, H., Roider, J., 2010. Change of morphological and functional characteristics of retinal pigment epithelium cells during cultivation of retinal pigment epithelium-choroid perfusion tissue culture. Ophthalmic Res. 43, 122–133.

Miura, Y., Roider, J., 2009. Triamcinolone acetonide prevents oxidative stress-induced tight junction disruption of retinal pigment epithelial cells. Graefes. Arch. Clin. Exp. Ophthalmol. 247, 641–649.

Miura, Y., Treumer, F., Klettner, A., Hillenkamp, J., Brinkmann, R., Birngruber, R., Roider, J., 2009. Laser power-dependent expression of vascular endothelial growth factor (VEGF) by porcine RPE after photocoagulation. Invest. Ophthalmol. Vis. Sci. ARVO Meet. Abstr. 50, 201.

Müller, H.H., Ptaszynski, L., Schlott, K., Debbeler, C., Bever, M., Koinzer, S., Birngruber, R., Brinkmann, R., Hüttmann, G., 2012. Imaging thermal expansion and retinal tissue changes during photocoagulation by high speed OCT. Biomed. Opt. Express 3, 1025–1046.

Nivon, M., Richet, E., Codogno, P., Arrigo, A.P., Kretz-Remy, C., 2009. Autophagy activation by NFkappaB is essential for cell survival after heat shock. Autophagy 5, 766–783.

Nowak, J.Z., 2013. Oxidative stress, polyunsaturated fatty acids-derived oxidation products and bisretinoids as potential inducers of CNS diseases: focus on age-related macular degeneration. Pharmacol. Rep. 65, 288–304.

Nowak, M.S., Jurowski, P., Grzybowski, A., Pastuszka, M., Kapica, A., Śmigielski, J., 2012. A prospective study on different methods for the treatment of choroidal neovascularization. The efficacy of verteporfin photodynamic therapy, intravitreal bevacizumab and transpupillary thermotherapy in patients with neovascular age-related macular degeneration. Med. Sci. Monit. 18, 374–380.

Obin, M., Shang, F., Gong, X., Handelman, G., Blumberg, J., Taylor, A., 1998. Redox regulation of ubiquitin-conjugating enzymes: mechanistic insights using the thiol-specific oxidant diamide. FASEB. J. 12, 561–569.

Odergren, A., Algvere, P.V., Seregard, S., Kvanta, A., 2008. A prospective randomized study on low-dose transpupillary thermotherapy versus photodynamic therapy for neovascular age-related macular degeneration. Br. J. Ophthalmol. 92, 757–761.

Oka, Y., Akagi, Y., Kinugasa, T., Ishibashi, N., Iwakuma, N., Shiratsuchi, I., Shirouzu, K., 2013. Heat-shock pre-treatment reduces liver injury and aids liver recovery after partial hepatectomy in mice. Anticancer. Res. 33, 2887–2894.

Pallepati, P., Averill-Bates, D.A., 2011. Mild thermotolerance induced at 40°C protects HeLa cells against activation of death receptor-mediated apoptosis by hydrogen peroxide. Free. Radic. Biol. Med. 50, 667–679.

Qin, S., Rodrigues, G.A., 2010. Differential roles of AMPKα1 and AMPKα2 in regulating 4-HNE-induced RPE cell death and permeability. Exp. Eye. Res. 91, 818–824.

Reichel, E., Berrocal, A.M., Ip, M., Kroll, A.J., Desai, V., Duker, J.S., Puliafito, C.A., 1999. Transpupillary thermotherapy of occult subfoveal choroidal neovascularization in patients with age-related macular degeneration. Ophthalmology 106, 1908–1914.

Roth, F., Bindewald, A., Holz, F.G., 2004. Keypathophysiologic pathways in age-related macular disease. Graefes. Arch. Clin. Exp. Ophthalmol. 242, 710–716.

Routt, S.M., Zhu, J., Zaleski, J.M., Dynlacht, J.R., 2011. Potentiation of metalloenediyne cytotoxicity by hyperthermia. Int. J. Hyperth. 27, 435–444.

Rudolf, M., Clark, M.E., Chimento, M.F., Li, C.M., Medeiros, N.E., Curcio, C.A., 2008. Prevalence and morphology of druse types in the macula and periphery of eyes with age-related maculopathy. Invest. Ophthalmol. Vis. Sci. 49, 1200–1209.
Schafer, F.Q., Buettner, G.R., 2001. Redox environment of the cell as viewed through the redox state of the glutathione disulfide/glutathione couple. Free. Radic. Biol. Med. 30, 1191–1212.
Schlingemann, R.O., 2004. Role of growth factors and the wound healing response in age-related macular degeneration. Graefes. Arch. Clin. Exp. Ophthalmol. 242, 91–101.
Schlott, K., Koinzer, S., Ptaszynski, L., Bever, M., Baade, A., Roider, J., Birngruber, R., Brinkmann, R., 2012. Automatic temperature controlled retinal photocoagulation. J. Biomed. Opt. 17, 061223.
Schutt, F., Davies, S., Kopitz, J., Holz, F.G., Boulton, M.E., 2000. Photodamage to human RPE cells by A2-E, a retinoid component of lipofuscin. Invest. Ophthalmol. Vis. Sci. 41, 2303–2308.
Sekiyama, E., Saint-Geniez, M., Yoneda, K., Hisatomi, T., Nakao, S., Walshe, T.E., Maruyama, K., Hafezi-Moghadam, A., Miller, J.W., Kinoshita, S., D'Amore, P.A., 2011. Heat treatment of retinal pigment epithelium induces production of elastic lamina components and antiangiogenic activity. FASEB. J. 26, 567–575.
Sharma, A., Sharma, R., Chaudhary, P., Vatsyayan, R., Pearce, V., Jeyabal, P.V., Zimniak, P., Awasthi, S., Awasthi, Y.C., 2008. 4-Hydroxynonenal induces p53-mediated apoptosis in retinal pigment epithelial cells. Arch. Biochem. Biophys. 480, 85–94.
Shrestha, R., Choi, T.Y., Chang, W., Kim, D.A., 2011. High-precision micropipette sensor for cellular-level real-time thermal characterization. Sensors 11, 8826–8835.
Singhal, S.S., Awasthi, S., Srivastava, S.K., Zimniak, P., Ansari, N.H., Awasthi, Y.C., 1995. Novel human ocular glutathione S-transferases with high activity toward 4-hydroxynonenal. Invest. Ophthalmol. Vis. Sci. 36, 142–150.
Söderberg, A.C., Algvere, P.V., Hengstler, J.C., Söderberg, P., Seregard, S., Kvanta, A., 2012. Combination therapy with low-dose transpupillary thermotherapy and intravitreal ranibizumab for neovascular age-related macular degeneration: a 24-month prospective randomised clinical study. Br. J. Ophthalmol. 96, 714–718.
Spitz, D.R., Dewey, W.C., Li, G.C., 1987. Hydrogen peroxide or heat shock induces resistance to hydrogen peroxide in Chinese hamster fibroblasts. J. Cell. Physiol. 131, 364–373.
Spitz, D.R., Sullivan, S.J., Malcolm, R.R., Roberts, R.J., 1991. Glutathione dependent metabolism and detoxification of 4-hydroxy-2-nonenal. Free. Radic. Biol. Med. 11, 415–423.
Sramek, C., Mackanos, M., Spitler, R., Leung, L.S., Nomoto, H., Contag, C.H., Palanker, D., 2011a. Non-damaging retinal phototherapy: dynamic range of heat shock protein expression. Invest. Ophthalmol. Vis. Sci. 52, 1780–1787.
Sramek, C., Leung, L.S., Leng, T., Brown, J., Paulus, Y.M., Schuele, G., Palanker, D., 2011b. Improving the therapeutic window of retinal photocoagulation by spatial and temporal modulation of the laser beam. J. Biomed. Opt. Feb 16 (2), 028004.
Stefánsson, E., 2006. Ocular oxygenation and the treatment of diabetic retinopathy. Surv. Ophthalmol. 51, 364–380.
Sternberg Jr., P., Davidson, P.C., Jones, D.P., Hagen, T.M., Reed, R.L., 1993. Protection of retinal pigment epithelium from oxidative injury by glutathione and precursors. Invest. Ophthalmol. Vis. Sci. 34, 3661–3668.
Theisen-Kunde, D., Tedsen, S., Doehn, C., Jocham, D., Kausch von Schmeling, I., 2011. Comparison between a 1.92-mum fiber laser and a standard HF-dissection device for nephron-sparing kidney resection in a porcine in vivo study. Lasers. Med. Sci. 26, 509–514.
Waldeck, A.R., Stocker, R., 1996. Radical-initiated lipid peroxidation in low density lipoproteins: insights obtained from kinetic modeling. Chem. Res. Toxicol. 9, 954–964.
Yanagihara, N., Moriwaki, M., Shiraki, K., Miki, T., Otani, S., 1996. The involvement of polyamines in the proliferation of cultured retinal pigment epithelial cells. Invest. Ophthalmol. Vis. Sci. 37, 1975–1983.
Yoshimura, N., Matsumoto, M., Shimizu, H., Mandai, M., Hata, Y., Ishibashi, T., 1995. Photocoagulated human retinal pigment epithelial cells produce an inhibitor of vascular endothelial cell proliferation. Invest. Ophthalmol. Vis. Sci. 36, 1686–1691.
Zarbin, M.A., 2004. Current concepts in the pathogenesis of age-related macular degeneration. Arch. Ophthalmol. 122, 598–614.
Zhang, H.J., Xu, L., Drake, V.J., Xie, L., Oberley, L.W., Kregel, K.C., 2003. Heat-induced liver injury in old rats is associated with exaggerated oxidative stress and altered transcription factor activation. FASEB. J. 17, 2293–2295.
Zhou, B., Wang, B., 2006. Pegaptanib for the treatment of age-related macular degeneration. Exp. Eye. Res. 83, 615–619.